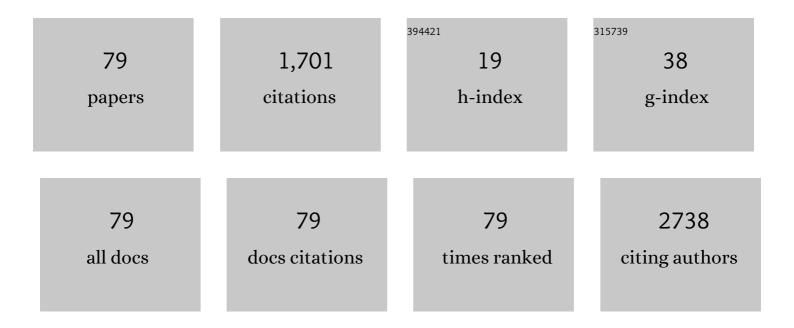
List of Publications by Year in descending order

Source: https://exaly.com/author-pdf/2169958/publications.pdf Version: 2024-02-01



Тім 7нн

#	Article	IF	CITATIONS
1	Head-to-head comparison of [68ÂGa]Ga-P16-093 and [68ÂGa]Ga-PSMA-617 in dynamic PET/CT evaluation of the same group of recurrent prostate cancer patients. European Journal of Nuclear Medicine and Molecular Imaging, 2022, 49, 1052-1062.	6.4	10
2	Kit-based preparation of [68Ca]Ga-P16-093 (PSMA-093) using different commercial 68Ge/68Ga generators. Nuclear Medicine and Biology, 2022, 106-107, 1-9.	0.6	4
3	Manipulating Electrocatalytic Polysulfide Redox Kinetics by 1D Core–Shell Like Composite for Lithium–Sulfur Batteries. Advanced Energy Materials, 2022, 12, .	19.5	47
4	New insights into the thermal degradation behavior of Hydroxypropyl-beta-cyclodextrin inclusion complexes containing carvacrol essential oil via thermogravimetric analysis. Journal of Thermal Analysis and Calorimetry, 2022, 147, 11301-11312.	3.6	9
5	Development and validation of a kit formulation of [68Ga]Ga-P15-041 as a bone imaging agent. Applied Radiation and Isotopes, 2021, 169, 109485.	1.5	8
6	Radiolabeling Optimization and Preclinical Evaluation of the New PSMA Imaging Agent [¹⁸ F]AlF-P16-093. Bioconjugate Chemistry, 2021, 32, 1017-1026.	3.6	8
7	The Novel Use of PVP K30 as Templating Agent in Production of Porous Lactose. Pharmaceutics, 2021, 13, 814.	4.5	12
8	A New Highly Deuterated [¹⁸ F]AV-45, [¹⁸ F]D15FSP, for Imaging β-Amyloid Plaques in the Brain. ACS Medicinal Chemistry Letters, 2021, 12, 1086-1092.	2.8	10
9	68Ga-labelled-exendin-4: New GLP1R targeting agents for imaging pancreatic β-cell and insulinoma. Nuclear Medicine and Biology, 2021, 102-103, 87-96.	0.6	5
10	Evaluating [68Ga]Ga-p14-032 as a Novel PET Tracer for Diagnosis Cerebral Amyloid Angiopathy. Frontiers in Neurology, 2021, 12, 702185.	2.4	4
11	Release Characteristics of an Essential Oil Component Encapsulated with Cyclodextrin Shell Matrices. Current Drug Delivery, 2021, 18, 487-499.	1.6	10
12	68Ga-P15-041, A Novel Bone Imaging Agent for Diagnosis of Bone Metastases. Frontiers in Oncology, 2021, 11, 766851.	2.8	4
13	An improved preparation of [¹⁸ F]AVâ€45 by simplified solidâ€phase extraction purification. Journal of Labelled Compounds and Radiopharmaceuticals, 2020, 63, 108-118.	1.0	5
14	[68Ga]Ga-HBED-CC-DiAsp: A new renal function imaging agent. Nuclear Medicine and Biology, 2020, 82-83, 17-24.	0.6	8
15	Systematic Analysis of Gibberellin Pathway Components in Medicago truncatula Reveals the Potential Application of Gibberellin in Biomass Improvement. International Journal of Molecular Sciences, 2020, 21, 7180.	4.1	10
16	Synthesis and Evaluation of ⁶⁸ Ga- and ¹⁷⁷ Lu-Labeled (<i>R</i>)- vs (<i>S</i>)-DOTAGA Prostate-Specific Membrane Antigen-Targeting Derivatives. Molecular Pharmaceutics, 2020, 17, 4589-4602.	4.6	10
17	Design, synthesis and evaluation of a novel glutamine derivative (2S,4R)-2-amino-4-cyano-4-[18F]fluorobutanoic acid. New Journal of Chemistry, 2020, 44, 9109-9117.	2.8	3
18	Dynamic PET/CT imaging of 18F-(2S, 4R)4-fluoroglutamine in healthy volunteers and oncological patients. European Journal of Nuclear Medicine and Molecular Imaging, 2020, 47, 2280-2292.	6.4	12

#	Article	IF	CITATIONS
19	Synthesis and evaluation of novel radioiodinated PSMA targeting ligands for potential radiotherapy of prostate cancer. Bioorganic and Medicinal Chemistry, 2020, 28, 115319.	3.0	5
20	Biodistribution, dosimetry, and temporal signal-to-noise ratio analyses of normal and cancer uptake of [68Ga]Ga-P15-041, a gallium-68 labeled bisphosphonate, from first-in-human studies. Nuclear Medicine and Biology, 2020, 86-87, 1-8.	0.6	13
21	A New [⁶⁸ Ga]Ga-HBED-CC-Bisphosphonate as a Bone Imaging Agent. Molecular Pharmaceutics, 2020, 17, 1674-1684.	4.6	20
22	VMAT2 imaging agent, D6-[18F]FP-(+)-DTBZ: Improved radiosynthesis, purification by solid-phase extraction and characterization. Nuclear Medicine and Biology, 2019, 72-73, 26-35.	0.6	8
23	Selfâ€Destruction of Cancer Induced by Ag 2 S Amorphous Nanodots. Small, 2019, 15, 1902945.	10.0	10
24	In Vivo Ester Hydrolysis as a New Approach in Development of Positron Emission Tomography Tracers for Imaging Hypoxia. Molecular Pharmaceutics, 2019, 16, 1156-1166.	4.6	9
25	In situ generation of biocompatible amorphous calcium carbonate onto cell membrane to block membrane transport protein – A new strategy for cancer therapy via mimicking abnormal mineralization. Journal of Colloid and Interface Science, 2019, 541, 339-347.	9.4	12
26	Conformational-transited protein corona regulated cell-membrane penetration and induced cytotoxicity of ultrasmall Au nanoparticles. RSC Advances, 2019, 9, 4435-4444.	3.6	23
27	Optimization of solid-phase extraction (SPE) in the preparation of [18F]D3FSP: A new PET imaging agent for mapping Al² plaques. Nuclear Medicine and Biology, 2019, 71, 54-64.	0.6	3
28	Rapid screening of nine unradiolabeled candidate compounds as PET brain imaging agents using cassette-wave microdosing and LC-MS/MS. Journal of Chromatography B: Analytical Technologies in the Biomedical and Life Sciences, 2019, 1121, 28-38.	2.3	1
29	Initial experience in synthesis of (<scp>2<i>S</i></scp> , <scp>4<i>R</i></scp>)â€4â€{ ¹⁸ F]fluoroglutamine for clinical application. Journal of Labelled Compounds and Radiopharmaceuticals, 2019, 62, 209-214.	1.0	2
30	Synthesis and preliminary evaluation of a novel glutamine derivative: (2S,4S)4-[18F]FEBGIn. Bioorganic and Medicinal Chemistry Letters, 2019, 29, 1047-1050.	2.2	9
31	A Targeting Membrane Injury Strategy via Calcification for the Inhibition of Leukemia Cells. ChemistrySelect, 2019, 4, 3642-3645.	1.5	3
32	(2S,4R)-4-[18F]Fluoroglutamine as a PET Indicator for Bone Marrow Metabolism Dysfunctional: from Animal Experiments to Clinical Application. Molecular Imaging and Biology, 2019, 21, 945-953.	2.6	9
33	Synthesis of novel technetium-99m tricarbonyl-HBED-CC complexes and structural prediction in solution by density functional theory calculation. Royal Society Open Science, 2019, 6, 191247.	2.4	3
34	Relationship of Carbon Isotope Discrimination with Biomass and Water Use Efficiency for Alfalfa in Northwestern China. Crop Science, 2019, 59, 400-412.	1.8	3
35	Novel thermostable enzymes from Geobacillus thermoglucosidasius W-2 for high-efficient nitroalkane removal under aerobic and anaerobic conditions. Bioresource Technology, 2019, 278, 73-81.	9.6	16
36	Multifunctional vanadium nitride@N-doped carbon composites for kinetically enhanced lithium–sulfur batteries. New Journal of Chemistry, 2018, 42, 5109-5116.	2.8	34

#	Article	IF	CITATIONS
37	Deuteriumâ€substituted 2â€{2′â€{(dimethylamino)methyl)â€4′â€{ ¹⁸ F](fluoropropoxy)phenylthio)benzenamine as a transporter imaging agent. Journal of Labelled Compounds and Radiopharmaceuticals, 2018, 61, 576-585.	serotonin	5
38	Synthesis and evaluation of a novel urea-based 68 Ga-complex for imaging PSMA binding in tumor. Nuclear Medicine and Biology, 2018, 59, 36-47.	0.6	32
39	Cobalt-Doped Vanadium Nitride Yolk–Shell Nanospheres @ Carbon with Physical and Chemical Synergistic Effects for Advanced Li–S Batteries. ACS Applied Materials & Interfaces, 2018, 10, 11642-11651.	8.0	102
40	Titanium nitride hollow nanospheres with strong lithium polysulfide chemisorption as sulfur hosts for advanced lithium-sulfur batteries. Nano Research, 2018, 11, 4302-4312.	10.4	81
41	NH3-SCR performance and the resistance to SO2 for Nb doped vanadium based catalyst at low temperatures. Journal of Environmental Sciences, 2018, 65, 306-316.	6.1	40
42	Deuterated 18 F-9-O-hexadeutero-3-fluoropropoxyl-(+)-dihydrotetrabenazine (D6-FP-(+)-DTBZ): A vesicular monoamine transporter 2 (VMAT2) imaging agent. Nuclear Medicine and Biology, 2018, 57, 42-49.	0.6	10
43	Imaging Brain Metastasis Patients With 18F-(2S,4R)-4-Fluoroglutamine. Clinical Nuclear Medicine, 2018, 43, e392-e399.	1.3	22
44	Self-Assembly Molecular Chaperone to Concurrently Inhibit the Production and Aggregation of Amyloid β Peptide Associated with Alzheimer's Disease. ACS Macro Letters, 2018, 7, 983-989.	4.8	17
45	Fluorine-18 labeled diphenyl sulfide derivatives for imaging serotonin transporter (SERT) in the brain. Nuclear Medicine and Biology, 2018, 66, 1-9.	0.6	4
46	PET Imaging of ¹⁸ F-(2 <i>S</i> ,4 <i>R</i>)4-Fluoroglutamine Accumulation in Breast Cancer: From Xenografts to Patients. Molecular Pharmaceutics, 2018, 15, 3448-3455.	4.6	18
47	Metabolic Imaging of Glutamine in Cancer. Journal of Nuclear Medicine, 2017, 58, 533-537.	5.0	63
48	Synthesis of novel PEG-modified nitroimidazole derivatives via "hot-click―reaction and their biological evaluation as potential PET imaging agent for tumors. Journal of Radioanalytical and Nuclear Chemistry, 2017, 312, 263-276.	1.5	9
49	Characterization and causes of land subsidence in Beijing, China. International Journal of Remote Sensing, 2017, 38, 808-826.	2.9	77
50	Photodynamic Therapy of Human Hepatoma Using Semiconductor Quantum Dots as Sole Photosensitizer. Particle and Particle Systems Characterization, 2017, 34, 1600413.	2.3	12
51	Engineering a highly thermostable and stress tolerant superoxide dismutase by N-terminal modification and metal incorporation. Biotechnology and Bioprocess Engineering, 2017, 22, 725-733.	2.6	3
52	Morphology Evolution on the Fracture Surface and Fracture Mechanisms of Multiphase Nanostructured ZrCu-Base Alloys. Materials, 2017, 10, 284.	2.9	1
53	Draft Genome Sequence of a Thermophilic Desulfurization Bacterium, <i>Geobacillus thermoglucosidasius</i> Strain W-2. Genome Announcements, 2016, 4, .	0.8	8
54	New 68Ga-PhenA bisphosphonates as potential bone imaging agents. Nuclear Medicine and Biology, 2016, 43, 360-371.	0.6	20

#	Article	IF	CITATIONS
55	One-step preparation of [18F]FPBM for PET imaging of serotonin transporter (SERT) in the brain. Nuclear Medicine and Biology, 2016, 43, 470-477.	0.6	10
56	Mitochondria-Mediated Protein Regulation Mechanism of Polymorphs-Dependent Inhibition of Nanoselenium on Cancer Cells. Scientific Reports, 2016, 6, 31427.	3.3	20
57	Fabrication of Various V ₂ O ₅ Hollow Microspheres as Excellent Cathode for Lithium Storage and the Application in Full Cells. ACS Applied Materials & Interfaces, 2016, 8, 17205-17211.	8.0	46
58	Improving the thermostability and stress tolerance of an archaeon hyperthermophilic superoxide dismutase by fusion with a unique N-terminal domain. SpringerPlus, 2016, 5, 241.	1.2	11
59	Contrasting correlation patterns between environmental factors and chlorophyll levels in the global ocean. Global Biogeochemical Cycles, 2015, 29, 2095-2107.	4.9	16
60	Synthesis of TEC-Substituted 4-(N-Methyl-N-Boc-amino)styrylpyridine as Key Precursor for Monodentate and Multidentate Imaging Agents for AβPlaques. Synthetic Communications, 2015, 45, 2740-2747.	2.1	3
61	Accumulation and elimination of iron oxide nanomaterials in zebrafish (Danio rerio) upon chronic aqueous exposure. Journal of Environmental Sciences, 2015, 30, 223-230.	6.1	55
62	Brain uptake of a non-radioactive pseudo-carrier and its effect on the biodistribution of [18F]AV-133 in mouse brain. Nuclear Medicine and Biology, 2015, 42, 630-636.	0.6	8
63	Genesis of Tropical Storm Debby (2006) within an African Easterly Wave: Roles of the Bottom-Up and Midlevel Pouch Processes. Journals of the Atmospheric Sciences, 2015, 72, 2267-2285.	1.7	6
64	Interfacial rheology and aggregation behaviour of amphiphilic CBABC-type pentablock copolymers at the air–water interface: effects of block ratio and chain length. RSC Advances, 2015, 5, 82869-82878.	3.6	7
65	Flue gas desulfurization gypsum by-products alters cytosolic Ca ^{2 +} distribution and Ca ²⁺ -ATPase activity in leaf cells of oil sunflower in alkaline soil. Journal of Plant Interactions, 2014, 9, 152-158.	2.1	7
66	Risk Assessment of Rotavirus Infection in Surface Seawater from Bohai Bay, China. Human and Ecological Risk Assessment (HERA), 2014, 20, 929-940.	3.4	9
67	Expanding the Scope of Fluorine Tags for PET Imaging. Science, 2013, 342, 429-430.	12.6	21
68	An improved preparation of [18F]FPBM: A potential serotonin transporter (SERT) imaging agent. Nuclear Medicine and Biology, 2013, 40, 974-979.	0.6	6
69	Ag2O–Bi2O3 composites: synthesis, characterization and high efficient photocatalytic activities. CrystEngComm, 2012, 14, 5705.	2.6	44
70	Study the pharmacokinetics of AVâ€45 in rat plasma and metabolism in liver microsomes by ultraâ€performance liquid chromatography with mass spectrometry. Biomedical Chromatography, 2012, 26, 666-671.	1.7	11
71	Rapid Detection of the Residual Kryptofix 2.2.2 Levels in [¹⁸ F]-Labeled Radiopharmaceuticals by Ultra-Performance Liquid Chromatography Tandem Mass Spectrometry. Analytical Letters, 2011, 44, 1197-1205.	1.8	2
72	Synthesis of Optically Pure 4-Fluoro-Glutamines as Potential Metabolic Imaging Agents for Tumors. Journal of the American Chemical Society, 2011, 133, 1122-1133.	13.7	144

#	Article	IF	CITATIONS
73	An improved radiosynthesis of [18F]AV-133: a PET imaging agent for vesicular monoamine transporter 2. Nuclear Medicine and Biology, 2010, 37, 133-141.	0.6	38
74	Acute toxicities of six manufactured nanomaterial suspensions to DaphniaÂmagna. Journal of Nanoparticle Research, 2009, 11, 67-75.	1.9	289
75	Synthesis and evaluation of 2-amino-dihydrotetrabenzine derivatives as probes for imaging vesicular monoamine transporter-2. Bioorganic and Medicinal Chemistry Letters, 2009, 19, 5026-5028.	2.2	28
76	The interconversion mechanism between TcO3+ and TcO2 + core of 99mTc labeled amine-oxime (AO) complexes. Theoretical Chemistry Accounts, 2008, 121, 271-278.	1.4	11
77	Complex fault tree analysis based on BDD route-based rules. , 2008, , .		0
78	Primary study of a novel Tc-tricarbonyl cocaine analogue as the potential DAT imaging agent. Science Bulletin, 2005, 50, 761-764.	1.7	0
79	Synthesis, separation and biodistribution of99mTc-CO-MIBI complex. Journal of Labelled Compounds and Radiopharmaceuticals, 2004, 47, 513-521	1.0	23